Different Equilibrium Stability Behavior of ScFv Fragments: Identification, Classification, and Improvement by Protein Engineering[†]

Arne Wörn and Andreas Plückthun*

Biochemisches Institut, Universität Zürich, Winterthurerstrasse 190, CH-8057 Zürich, Switzerland

Received January 27, 1999; Revised Manuscript Received March 24, 1999

ABSTRACT: A classification of scFv fragments concerning their unfolding/refolding equilibria is proposed. It is based on the analysis of different mutants of the levan-binding A48 scFv fragment and the HER-2 binding 4D5 scFv fragment as well as a "hybrid" scFv carrying the V_L domain of 4D5 and the V_H domain of an A48 mutant. The denaturant-induced unfolding curves of the corresponding scFv fragments were measured and, if necessary for the classification, compared with the denaturation of the isolated domains. Depending on the relative intrinsic stabilities of the domains and the stability of the interface, the different scFv fragments were grouped into different classes. We also demonstrate with several examples how such a classification can be used to improve the stability of a given scFv fragment, by concentrating engineering efforts on the "weak part" of the particular molecule, which may either be the intrinsic stability of V_L, of V_H, or the stability of the interface. One of the scFv fragments obtained by this kind of approach is extremely stable, starting denaturation only at about 7 M urea. We believe that such extremely stable frameworks may be very suitable recipients in CDR grafting experiments. In addition, the thermodynamic equilibrium stabilities of seven related A48 scFv mutants covering a broad range of stabilities in urea unfolding were shown to be well correlated with thermal aggregation properties measured by light scattering and analytical gel filtration.

Improving the stability of scFv[1] fragments (*1*, *2*) for biotechnological or medical applications is a major challenge for protein engineers. The relatively easy production of scFv fragments in bacteria (*3*, *4*) and, compared with the parental mAb, their almost unchanged monomeric binding affinity (*1*, *4*, *5*) explain their increasing importance in many fields. ScFv fragments with increased stability were shown to have improved in vivo properties (ref *6*; Willuda et al., manuscript submitted for publication). The molecular basis of observed differences in stability between different scFv fragments is, however, not really clear. An indispensable prerequisite for the future engineering of stability of these proteins is therefore to understand their equilibrium denaturation and their aggregation properties in greater detail.

One of the possibilities to examine scFv stabilities is to analyze their denaturant-induced equilibrium unfolding (*7*), by following the spectroscopic properties of the protein (*8*), such as tryptophan fluorescence. However, this denaturant-induced equilibrium unfolding of scFv fragments is not necessarily a simple two-state process, which would only involve the native and the completely denatured state of the protein. Instead, intermediate species may accumulate at equilibrium, involving one native and one denatured domain or interacting domains which are only partially unfolded. We have demonstrated the presence of such an intermediate with native V_H and denatured V_L domain before in the case of the A48cys(H-K66R/N52S) scFv fragment (*9*).

In this study, we use two model systems, the scFv fragments A48 and 4D5. The A48 scFv is derived from a levan binding antibody, ABPC48, naturally missing the V_H intradomain disulfide (*10*−*12*). In previous work, this scFv fragment has been produced in a cysteine-restored form $A48^{++}$ (carrying both intradomain disulfides, denoted "A48cys" in the earlier study) (*11*) and in a completely cysteine-free form (*12*). In the meantime, we have created and analyzed many further mutants of the A48 scFv fragment. The analysis of these mutants and of the $p185^{HER2-ECD}$-binding 4D5 scFv fragment (*13*, *14*), taken together with our previous results for some A48 scFv mutants (*9*), allows us to finally assemble a general model and to propose a classification of the denaturation behavior of scFv fragments. This classification puts scFv fragment into different classes, depending on the part of the scFv fragment which is limiting for the total stability of the protein. The stability-limiting property of the scFv fragment can either be the intrinsic stability of either one of its domains (V_H or V_L) or, alternatively, the stability of the interface.

[†] This study was funded by the Schweizerische Nationalfonds Grant 31-47302.96 and by a predoctoral fellowship to A.W. from the Fonds der Deutschen Chemischen Industrie.

* To whom correspondence should be addressed. Fax (+41-1) 635 5712. E-mail: plueckthun@biocfebs.unizh.ch.

[1] Abbreviations: $A48^{--}$, variant of the A48 scFv fragment lacking both intradomain disulfide bonds; $A48^{++}$, variant of the A48 scFv fragment carrying both intradomain disulfides; BBS, borate-buffered saline; CDR, complementarity determining region; GdnHCl, guanidinium hydrochloride; mAb, monoclonal antibody; $p185^{HER2-ECD}$, extracellular domain of human epidermal growth factor receptor 2; scFv, single-chain Fv fragment of an antibody; scFv (SS), single-chain Fv variant carrying an interdomain disulfide bond between the mutated framework positions H44 and L100; T_{agg}, aggregation temperature; V_H, variable domain of the heavy chain; V_L, variable domain of the light chain.

10.1021/bi9902079 CCC: $18.00
Published on Web 06/15/1999

The present study combines new data with previous studies on the A48 scFv (*9*). The combined data are analyzed to show examples of several different types of unfolding behavior in order to assemble a general model. The practical benefit of such a classification is that it can help to increase the stability of a given scFv fragment by first identifying and then improving its stability limiting part. This approach is demonstrated in the present study with several examples.

A further point investigated is the question of how the thermodynamic stability of scFv fragments, measured by equilibrium unfolding, correlates with their irreversible thermal aggregation properties. This question is of more practical relevance, because scFv fragments often tend to aggregate upon concentration, heating, or longer storage, and this aggregation tendency is one limiting factor for medical or biotechnological applications of scFv fragments. The comparison of stability against denaturant and thermal aggregation properties was performed by analyzing seven mutants of the A48 scFv fragment which cover a broad range of stabilities, yet differing between each other by only a few point mutations. This was possible because some mutants are lacking one or both of the conserved intradomain disulfide bonds, and several of these A48 fragments were stabilized by additional point mutations. The analysis of these scFv fragments included their denaturant-induced equilibrium unfolding, their aggregation temperature measured by light scattering at 500 nm, and their aggregation after prolonged incubation at 37 °C (which is below the actual aggregation temperature of all scFv fragments under investigation), monitored by analytical gel filtration.

EXPERIMENTAL PROCEDURES

ScFv Fragments Analyzed. Most of the scFv fragments studied (Figure 1) were derived from the A48 scFv fragment, either in its completely cysteine-free form lacking both intradomain disulfides ($A48^{--}$), in its cysteine-restored form, containing the disulfides in both V_H and V_L ($A48^{++}$) (*11*), or in its "wild-type" form lacking only the V_H disulfide ($A48^{-+}$). Several stabilizing mutations were introduced into these scFv fragments in different combinations. The mutations H-K66R and H-N52S in the heavy chain have been described in refs *9* and *12*. The mutation H-Y92V in the heavy chain can only be introduced into the disulfide-free or the wild-type variants, because residue H92 is one of the positions forming the conserved intradomain disulfide bond. The L-T8P mutation in the light chain is a substitution toward the κ-consensus sequence [classification of V_H subgroups and numbering according to Kabat et al. (*15*)] and was shown to stabilize a different scFv fragment before (*16*).

All scFv fragments as well as the isolated domains under investigation are schematically represented in Figure 1 and described here: $A48^{--}$(H-K66R) [named $A48^{--}$(H1), the double minus denoting that it is disulfide-free and the parenthesis indicating that it carries one stabilizing heavy chain mutation], $A48^{--}$(H-K66R/N52S) [named $A48^{--}$(H2)], $A48^{--}$(H-K66R/N52S/Y92V) [named $A48^{--}$(H3)], $A48^{--}$(H-K66R/N52S/Y92V)(L-T8P) [named $A48^{--}$(H3L1)], $A48^{--}$ (H-K66R/N52S)(SS) [named $A48^{--}$(H2)(SS)—this protein carries an interface disulfide bond between the mutated framework positions Gly H44 and Gly L100, which are known to be in a suitable orientation to bridge the interface, when replaced by cysteines (*17*)], A48wt(H-K66R) [named $A48^{-+}$(H1)], $A48^{++}$(H-K66R/N52S) [named $A48^{++}$(H2)], and $A48^{++}$(H-K66R/N52S)(L-T8P) [named $A48^{++}$(H2L1)]. Additionally, the isolated disulfide-contain-

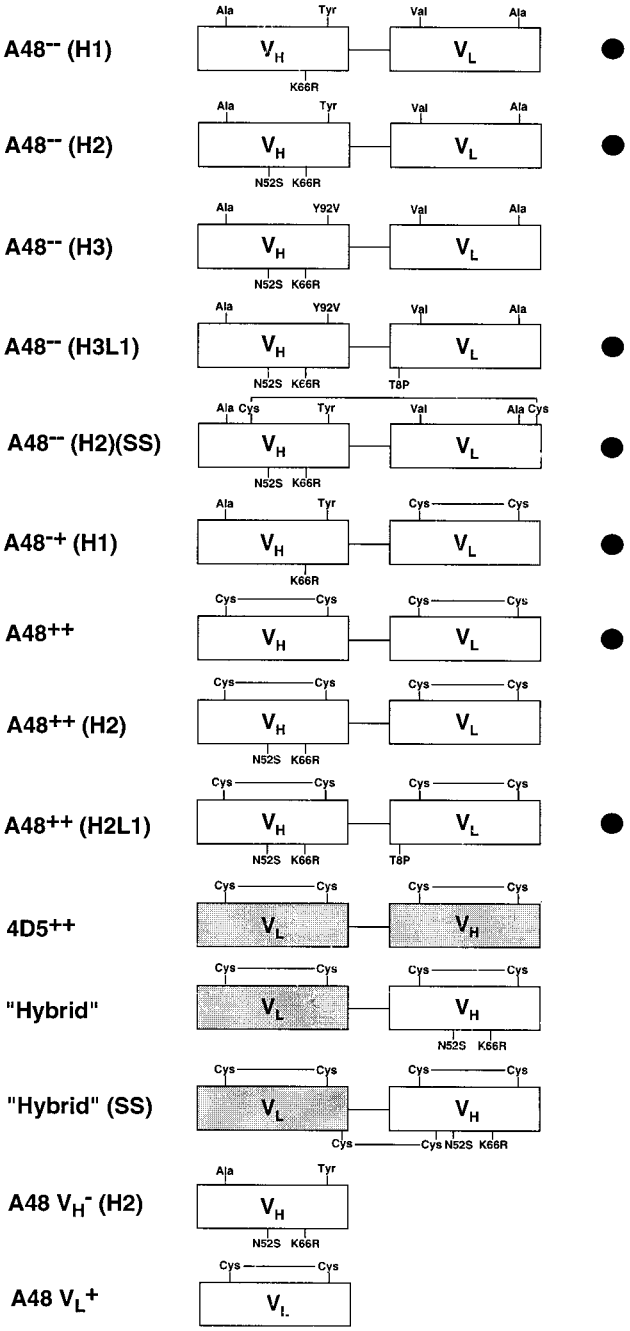

FIGURE 1: Schematic representation of the different scFv fragments and isolated domains under investigation in this study. The mutants labeled "$A48^{--}$" are completely cysteine free, those termed "$A48^{++}$" have both intradomain disulfide bonds in V_H and V_L and the mutant called "$A48^{-+}$" has the intradomain disulfide in V_L but not in V_H. Stabilizing point mutations are indicated. The *number* of stabilizing mutations in V_H and V_L in the particular mutants is attached to its name. The scFv fragments labeled "(SS)" have an interface disulfide bond between framework positions H44 and L100, which were mutated to Cys residues in these particular scFv fragments. 4D5-derived domains are shaded. The variant called "hybrid" scFv carries the V_L domain of the 4D5 scFv fragment linked to the V_H domain of the $A48^{++}$(H2) scFv fragment. Those mutants that have been analyzed for their thermal aggregation properties are labeled with a black dot.

ing V_L domain of the antibody A48 without additional mutations (named A48V_L^+) and the disulfide-free V_H domain with the H-K66R/N52S mutations [named A48V_H^-(H2)] have been examined. The seven selected A48 mutants additionally analyzed for their thermal aggregation properties are emphasized in Figure 1 with a black dot.

While four of the A48 mutants have been described before [A48^{++}, A48^{++}(H2), A48^{-+} (H1), and A48V_L^+ (*9*, *11*)], we need to include these denaturation transitions in the corresponding overlays, to be able to explain the proposed scFv classification.

Furthermore, the 4D5 scFv fragment (*13*, *14*) has been used as a representative example for one of the proposed scFv classes. Additionally, a "hybrid" scFv with the V_L domain of the 4D5 linked to the V_H domain of the A48^{++}(H2) has been analyzed, as well as its interface disulfide bridged derivative "hybrid" scFv (SS), where again Gly H44 of the A48^{++}(H2) V_H domain and Gln L100 of the 4D5 V_L domain were mutated to cysteines.

Protein Expression and Purification. Protein expression and affinity purification of the A48 scFv fragments was performed as described before (*9*, *11*, *12*). All A48^{--}-derived mutants, including the one carrying the interface disulfide, the mutant A48^{-+}(H1), and the isolated A48V_H^-(H2) domain were cloned into the vector pTFT74 (*18*, *19*) and expressed as cytoplasmic inclusion bodies in *Escherichia coli* BL21DE3 [F^-, *ompT*$^-$, $r_B^-m_B^-$ (λimm21, *lac*I, *lac*UV5, *T7 pol*, *int*)] (*20*). Refolding and purification of the interface-bridged variant A48^{--}(H2)(SS) and the A48^{-+}(H1) was performed exactly as described for the A48 wt-derived mutants before (*9*). Refolding and purification of the A48V_H^-(H2) domain was analogous to the published procedure for the A48I-1(V_H) domain (*9*), and all the remaining A48^{--}-derived mutants were refolded and affinity purified as described for the disulfide-free A48 mutants before (*12*).

Periplasmic expression in *E. coli* JM83 [λ^-, *ara*, Δ(*lac*, *proAB*), *rpsL*, *thi*, Φ80, *dlacZ*ΔM15] (*21*) and purification of the scFv fragments A48^{++}, A48^{++}(H2), and A48^{++}(H2L1) was carried out as described before (*9*). The 4D5 scFv fragment, the "hybrid" scFv, and its interface-bridged variant were expressed periplasmically and purified as described for the disulfide-containing 4D5 scFv fragment (*14*).

All A48-derived mutants were in a V_H-linker-V_L orientation, carrying an N-terminal FLAG (*22*) and a C-terminal Myc- and His-tag (*11*). The 4D5-derived mutants as well as the "hybrid" scFv fragments with and without the interface disulfide were in a V_L-linker-V_H orientation, with the same 20-mer nonrepetitive peptide linker (*23*) and with the same tags. Semiquantitative comparisons of scFv stabilities are only performed between scFv fragments in identical orientations.

Urea- and GdnHCl-Induced Unfolding/Refolding Equilibria. Solvent-induced denaturation was followed by the intrinsic fluorescence emission spectra of the proteins. Excitation was at 280 nm. Measurements were performed and analyzed as described before (*12*). All A48-derived mutants were measured in BBS buffer (50 mM sodium borate, pH 8.0, and 150 mM NaCl), the 4D5 and the "hybrid" scFv fragments were measured in 40 mM Tris, pH 8.0, and 150 mM NaCl. It was verified that this difference in buffer did not influence the transition curves (data not shown). Depending on the stability of the analyzed mutants, either urea or the stronger denaturant GdnHCl were used for the stability measurements (Figure 2). To demonstrate the extraordinary stability of the "hybrid" scFv (SS) in urea, transition curves of this scFv fragment were measured in both GdnHCl and urea. Proposed scFv classes are described in Figure 3.

Limited Protease Digestion Studies. To characterize an equilibrium intermediate present at 2 M GdnHCl, limited thermolysin digestion (*24*), subsequent SDS−PAGE (Figure 4), blotting, and N-terminal sequencing of the accumulating digestion bands were performed with the 4D5 scFv fragment as described for the A48cys(H-K66R/N52S) fragment before (*9*). The digestion was performed in 2 M GdnHCl—corresponding to the expected intermediate with native V_L and denatured V_H in the 4D5 scFv fragment. A ratio of thermolysin to scFv of 1:100 (w/w) was used and the final scFv concentration in the digestion mix was 850 μg/mL.

Determination of Aggregation Temperature. The seven A48 mutants indicated in Figure 1 were also analyzed for their thermal aggregation properties. Their temperature of aggregation was determined by light scattering similar as described previously (*25*). A Shimadzu RF-5000 spectrofluorimeter was used. Excitation and emission wavelength were 500 nm. The scFv samples were measured in BBS buffer at 300 μg/mL (about 10 μM, with the exact molar concentration differing minimally between the investigated point mutants). After filtering through 0.2 μm Millipore filters, they were heated in a 2 mL quartz cuvette in a volume of 1.7 mL and continuously stirred with a small magnetic stirrer. The temperature was controlled by a programmable circulating water bath, and the exact actual temperature in the cuvette was determined with blanks, using a small temperature sensor in the cuvette to calibrate the water bath. A temperature gradient of 0.5 °C/min was applied starting from 25 °C up to the temperature which was necessary to get the maximum intensity measurable by the spectrofluorimeter. Intensities were measured every 0.2−0.5 °C (in general, more points were measured when the scattered intensity started to rise). Each intensity point depicted in the plots (Figure 5, panels b and c) was averaged over 10 measured intensity values. The time period necessary for collection of this set of 10 data points was about 10−15 s, and therefore only a negligible intensity change occurred due to the concomitant rise in temperature (about 0.1 °C). The aggregation temperature was obtained from the intensity versus temperature plot by linear extrapolation to the temperature axis after correcting for minor background scattering present from the beginning of the measurement. This was done by linear fitting of the intensity values in the pretransition region and setting the scattered intensity at $T = 25$ °C to zero for all variants. To get an objective value for the aggregation temperatures, all points exceeding intensity values of 400 (see Figure 5) were used for linear extrapolation. All measurements were performed in duplicate or triplicate, and averaged values are given (see Figure 5c, as an example for a representative triplicate measurement).

Analytical Gel Filtration. Analytical gel filtrations of the seven selected A48 mutants (see above) were performed with a SMART-system (Pharmacia), using a Superdex-75 column. All measurements were carried out in BBS buffer with 0.005% Tween-20. The respective scFv fragments were injected at 300 μg/mL (about 10 μM) in a volume of 50 μL.

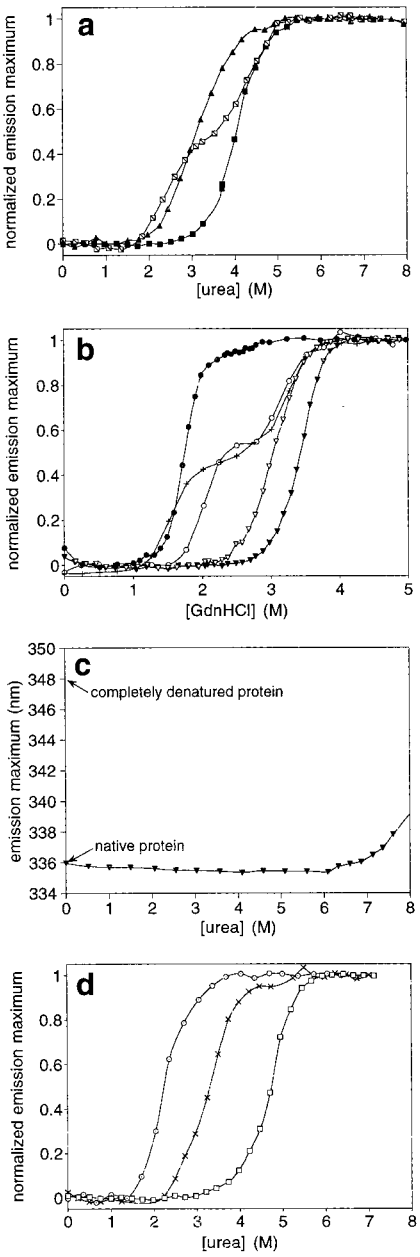

FIGURE 2: Denaturant induced equilibrium unfolding of different scFv fragments. Unfolding was followed by the change in fluorescence emission maximum (excitation 280 nm). For better comparison, unfolding curves are normalized with the exception of 2c, where the emission maximum raw data are shown, because normalization was not possible due to the lack of a complete transition and a post-transition region. (a) *Effect of stabilizing first V_H, then V_L.* Unfolding curves of A48^{--}(H2) (▲), A48^{--}(H3) (◹), and A48^{--}(H3L1) (■). (b) *Comparison of "hybrid" scFv with and without interface disulfide bond and the constituent scFv fragments.* Unfolding curves of 4D5 (●), A48^{++}(H2) (+), A48^{++}(H2L1) (○), "hybrid" scFv consisting of the V_L domain of 4D5 and the V_H domain of A48^{++}(H2) (▽), "hybrid" scFv (SS) with interface disulfide bond between the mutated positions H44 and L100 (▼). (c) *Demonstration of the extraordinary stability of "hybrid" scFv (SS).* The scFv fragment starts denaturing only at about 7 M urea. (d) *Effect of an interface disulfide bond on an scFv fragment with intrinsically very unstable domains.* Unfolding curves of A48^{--}(H2)-(SS) scFv (□), its A48V_H^-(H2) domain (×) and its A48V_L^+ domain (⊙). The isolated V_L domain carries the intradomain disulfide, differing from the V_L domain in the A48^{--}(H2)(SS) scFv. Both isolated domains denatured significantly earlier than the scFv fragment.

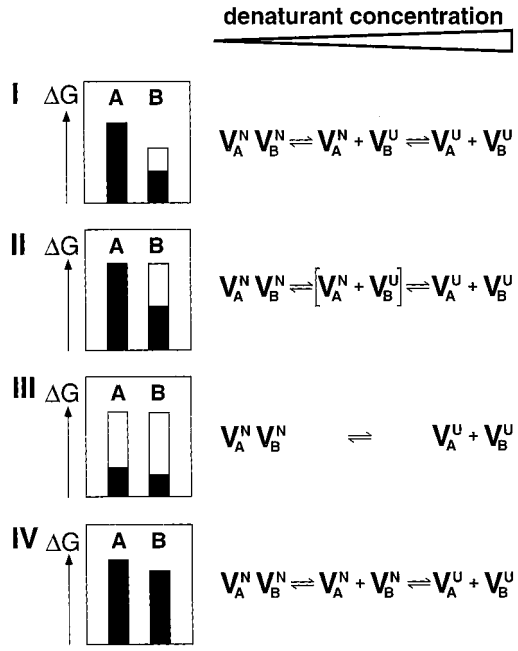

FIGURE 3: Schematic representation of possible unfolding equilibria in scFv fragments. A and B represent the respective domains of the scFv fragment (either V_H or V_L) and A is defined as the more stable domain. Δ*G* indicates the relative stability. *Intrinsic* stabilities are marked as black bars, *extrinsic* stability contributions provided by the V_H−V_L interface are represented by white bars. The superscripts N and U represent native and unfolded states of the corresponding domain, respectively. (I) The intrinsic stability of one domain is much higher than the total stability of the other domain. An equilibrium intermediate with one native and one denatured domain accumulates at intermediate denaturant concentration. (II) The intrinsic stability of one domain is in the same range as the total stability of the other domain. The transition to case I is gradual. The intermediate species with one native and one denatured domain will be less populated and well defined than in case I. (III) Two intrinsically relatively unstable domains are linked by a very stable interface. The breaking up of the interface is accompanied by the immediate denaturation of both domains. No intermediate accumulates at equilibrium, the transition is two-state. (IV) Two intrinsically very stable domains are linked by a weak interface. The interface disrupts at relatively low denaturant concentration, and the two domains remain native. Only at higher denaturant concentration the isolated domains will unfold in the order which is solely dependent on their intrinsic stabilities.

The column was calibrated in the same buffer with alcohol-dehydrogenase (150 kDa), bovine serum albumin (66 kDa), carbonic anhydrase (29 kDa), and cytochrome *c* (12.4 kDa) as molecular mass standards. The amount of monomeric protein was quantitated by integrating the peak eluting at about 1.2 mL, which corresponds to monomeric scFv fragment. All scFv fragments were analyzed before the temperature incubation, immediately after 20 h of incubation at 37 °C, and again after 120 h incubation at 37 °C. The incubated samples were centrifuged for 5 min at 14000*g* before applying them to the column to remove large aggregates which might block the Superdex-75 column.

RESULTS

Protein Expression and Purification. The purification yields of the periplasmically expressed A48 scFv fragments were about 1.2 mg for A48^{++} and A48^{++}(H2), respectively, and 0.7 mg for A48^{++}(H2L1) per liter of *E. coli* JM83. The scFv fragments expressed as cytoplasmic inclusion bodies

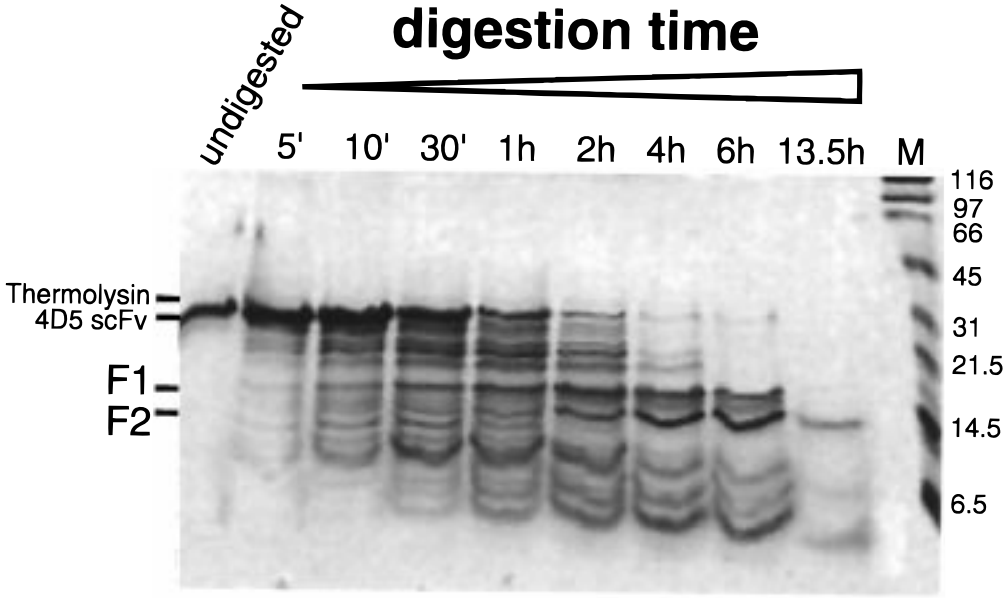

FIGURE 4: Limited thermolysin digestion of 4D5 scFv fragment in the presence of 2 M GdnHCl (which is the concentration where V_H appears to be denatured and V_L seems to be folded, based on the transition curve). Even after long digestion time, mainly two fragments (labeled F1 and F2) which convert to one fragment (F2) after 13.5 h digestion accumulated, which both had the same N-terminus of the 4D5 V_L domain—indicating that the 4D5 V_L is indeed still native under these conditions. Note that the marker band is distorted by the GdnHCl present in the samples running in the neighboring lanes.

yielded between 20 and 40 mg of purified protein/L *E. coli* BL21 after in vitro refolding. Only the mutant A48^{--}(H3L1) had a significantly lower yield, and only about 2 mg of purified scFv fragment was obtained upon refolding of this protein per liter of culture. The purification yield for the isolated A48V_H^-(H2) was 2.9 mg/L *E. coli* BL21. Purification of the 4D5 scFv, secreted into the periplasm, resulted in about 10 mg of pure protein/L *E. coli* JM83 (*14*); the "hybrid" scFv was even better expressed in the periplasm, yielding up to 13 mg of scFv protein after purification from 1 L of culture. The purification yield of the "hybrid" scFv was, however, dramatically reduced to about 450 μg/L *E. coli* JM83, when the interface disulfide bridge between H44 and L100 was inserted.

Urea- and GdnHCl-Induced Unfolding/Refolding Equilibria. The normalized denaturation curves of all investigated mutants used for the scFv classification are depicted in Figure 2, panels a, b, and d, while the curves of those A48 mutants additionally analyzed for their thermal aggregation properties are shown together with the respective aggregation data in Figure 5. Note that some curves are presented in both figures. While the shift in fluorescence emission maximum indicates the transition regions and the respective plateaus before and after the transition, it does not quantitatively reflect the fraction of unfolded protein in those cases which are not two-state transitions. The *y*-axis is therefore labeled "normalized emission maximum", rather than "fraction unfolded". The reason for nevertheless presenting the data in this normalized form is that this representation allows us to compare the position of different curves better than if the raw emission maximum data were shown.

For the very stable mutants in Figure 2b, the stronger denaturant GdnHCl was used, while urea was used to induce unfolding of the less stable proteins in Figures 2, panels a and d, and 5a. However, our interpretation does not require a quantitative comparison between urea and GdnHCl curves. The emission maximum of all the mutants derived from A48^{--} was close to 333 nm for the native proteins, while the A48^{++} scFv fragments and the A48^{-+}(H1) had an emission maximum of 336 nm. This shift in the emission maximum can be explained by the presence or the absence of the V_L intradomain disulfide bond, which is known to quench the fluorescence emission of the Trp residue in its vicinity (*26*). The 4D5 scFv fragment as well as the "hybrid" scFv fragment had their fluorescence emission maximum at 336 nm, demonstrating that also in the "hybrid" scFv the interface between V_H and V_L had been formed. If the interface had not formed in this variant, the spectrum of the native "hybrid" scFv would be an algebraic sum of native V_H and V_L, which would clearly result in a higher maximum than 336 nm (*27*), because of the exposed interface Trp residues of V_H and the subsequent red-shift in the fluorescence emission maximum. The fully denatured proteins had all emission maxima around 348−350 nm, consistent with the emission maximum of Trp in aqueous solution (*28*).

Figure 2a shows an overlay of the denaturation curves corresponding to the three related scFv fragments A48^{--}(H2), A48^{--}(H3), and A48^{--}(H3L1) which differ only in stabilizing point mutations. The A48^{--}(H2) scFv fragment showed a relatively flat transition (filled triangles compared to filled squares). We interpret this as the two domains denaturing slightly one after the other. Upon addition of the mutation H-Y92V, which stabilizes V_H, a clear step appeared in the denaturation curve of this scFv fragment (striped open squares), and the upper part of the denaturation curve in A48^{--}(H3) was shifted by about 0.6 M urea to higher urea concentrations. When the V_L-stabilizing mutation L-T8P was introduced into the latter scFv fragment as well, generating the fragment A48^{--}(H3L1), this step disappeared (filled squares), because the lower part of the denaturation transition was now shifted to higher urea concentrations, while the upper part remained unchanged.

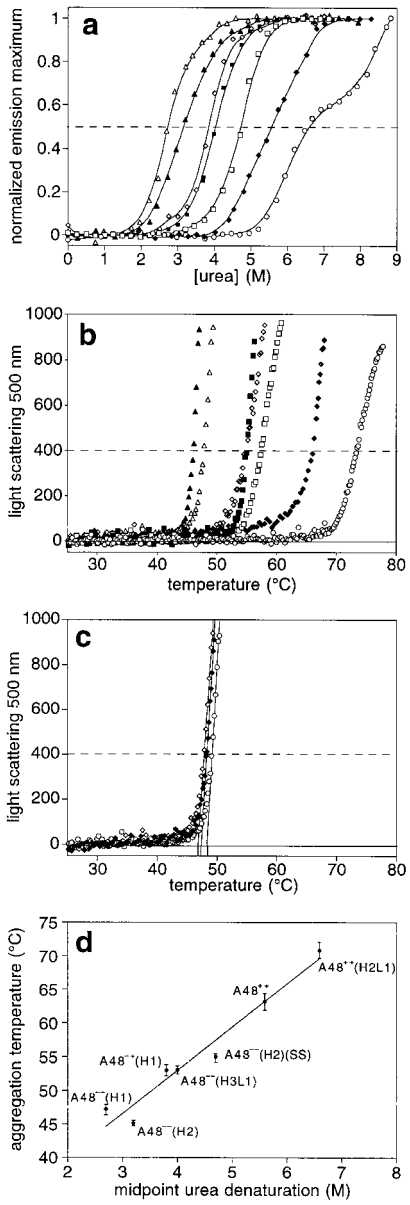

FIGURE 5: Correlation between urea denaturation midpoint and aggregation temperature in A48 scFv fragments. (a) Normalized urea equilibrium unfolding curves. Unfolding was followed by the change in fluorescence emission maximum (excitation 280 nm). The broken line indicates an emission maximum halfway between native and fully denatured state. The particular scFv fragments are indicated as follows: A48^{--}(H1) (△), A48^{--}(H2) (▲), A48^{-+}(H1) (◇), A48^{--}(H3L1) (■), A48^{--}(H2)(SS) (□), A48^{++} (◆), and A48^{++}(H2L1) (○). (b) Thermal aggregation of the different A48 scFv fragments, measured by light scattering at 500 nm as a function of the actual temperature in the cuvette. The same symbols as in panel a are used for the different A48 scFv mutants. Representative examples of the aggregation curves, which were performed in duplicate or triplicate for all proteins, are shown. (c) Demonstration of reproducibility of aggregation measurements. The three measurements [number 1 (◇), number 2 (◆) and number 3 (○)] for A48^{--}(H1) were performed on different days. (d) Overall linear correlation of aggregation temperature and midpoint in urea unfolding curves of different mutant A48 scFv fragments. Each point represents one of the seven A48 mutants under investigation. The numeric values are summarized in Table 1. They are extracted from panel a and from averaged aggregation temperatures, obtained from two or three independent measurements for each protein, analogous to the one depicted in panel b. Error bars indicate the upper and lower limit of replicate measurements. The linear fit had a correlation factor of $R = 0.97$.

In Figure 2b, an overlay of five different GdnHCl denaturation curves is depicted. The denaturation curves of the A48^{++}(H2) and A48^{++}(H2L1) fragments both showed clear steps in their transition curves. It can thus be seen that the additional L-T8P mutation did result in a shift of the lower curve to higher denaturant concentrations—similar as seen in Figure 2a for the fragment A48^{--}(H3) and A48^{--}(H3L1). However, in contrast to A48^{--}(H3L1), a clear intermediate species remained in the A48^{++}(H2L1) (open circles). The denaturation curve of the scFv fragment 4D5 (filled circles) did not show such an obvious step. However, a very small step is apparent at about 2−2.5 M GdnHCl in the region where many data points were collected. Several pieces of supporting evidence (see below) suggest that this is a real transition, in which V_L is denaturing, while V_H is already denaturing at about 1.5 M GdnHCl.

Since the small step in the 4D5 unfolding curve is believed to represent an equilibrium intermediate with native V_L and denatured V_H (see below) and since the clearly visible steps in the A48^{++}-derived mutants represent intermediates with native V_H and denatured V_L (*9*), the "hybrid" scFv consisting of the very stable V_L domain of 4D5 and the very stable V_H domain of A48^{++}(H2) should then be extraordinarily stable. Indeed, this "hybrid" scFv fragment turned out to be not only extremely well expressed in the periplasm (13 mg/L after purification), but also to be highly stable, starting denaturation only at about 2.5 M GdnHCl with a midpoint at 3.0 M GdnHCl (Figure 2b, open triangles). This "hybrid" scFv could be even further stabilized by introducing the interface disulfide bond, resulting in a further shift of the denaturation curve by about 0.4 M GdnHCl to higher denaturant concentration (Figure 2b, filled triangles), but at the expense of lower expression yields (see above). Figure 2c underlines the extraordinary stability of the "hybrid" (SS) scFv fragment. It starts denaturing only at about 7 M urea, a concentration where many scFv fragments have already finished their transition and are fully denatured. In this particular case, the raw data of the emission maximum are shown, because the curve could not be normalized due to the absence of the transition and post-transition region.

The transition curve of the other interface disulfide bridged variant studied, A48^{--}(H2)(SS) (Figure 2d, open squares), is overlaid with the curves corresponding to its isolated V_H domain (crosses) and its V_L domain (dotted open circles), which, however, carries an intradomain disulfide bond. Note that the same V_L domain without the intradomain disulfide, as present in A48^{--}(H2)(SS), could not be successfully expressed on its own, probably due to its low stability (data not shown), as it would be expected to have an even earlier transition than the V_L domain with the intradomain disulfide. The transition of the A48^{--}(H2)(SS) fragment occurred with a midpoint at about 4.8 M urea and therefore significantly later than the transition of either of its constituting domains.

The seven different A48 mutants used for comparison with thermal aggregation properties (Figure 5) denatured at widely different urea concentrations, from a denaturation midpoint of 2.7 M for the scFv fragment A48^{--}(H1) to 6.6 M for the cysteine-restored variant A48^{++}(H2L1) (Figure 5a, see Table 1 for exact numbers of denaturation midpoints).

Limited Protease Digestion Studies. After prolonged thermolysin digestion of the 4D5 scFv fragment in the presence of 2 M GdnHCl, mainly two fragments of about

Table 1: Summary of Urea Denaturation Midpoints, Averaged Aggregation Temperatures out of Three Independent Measurements for Each Protein and Percentage Monomeric scFv Fragment after 20 and 120 h of Incubation at 37 °C for Seven A48 scFv Fragments

ScFv fragment	midpoint urea denaturation (M)	averaged aggregation temp (°C)	monomeric scFv after 20 h at 37 °C (%)	monomeric scFv after 120 h at 37 °C (%)
A48^{--}(H1)	2.7	47.2	30.1	0
A48^{--}(H2)	3.2	45.1	1.7	0
A48^{-+}(H1)	3.8	53.0	80.7	41.2
A48^{--}(H3L1)	4.0	53.0	84.5	29.3
A48^{--}(H2)(SS)	4.7	55.0	85.4	37.3
A48^{++}	5.6	63.2	99.2	90.3
A48^{++}(H2L1)	6.6	70.8	94.0	91.8

14 and 16 kDa accumulated (Figure 4). N-Terminal sequencing confirmed that they both were N-terminal fragments of the scFv, starting with the N-terminus of the 4D5 V_L domain. After further digestion overnight, only the lower molecular mass fragment F2 remained visible, although clearly reduced in intensity.

Determination of Aggregation Temperature. As soon as protein aggregation started upon increasing the temperature, the scattered intensity at 500 nm rose rapidly and significantly, until the maximum intensity measurable by the fluorimeter was reached (Figure 5b). Some slight scattered intensity was present from the beginning, probably caused by occasional dust particles present in the protein samples despite filtering the samples with 0.2 μm filters prior to the measurement. This initial background scattering of the different samples was subtracted, and thus the scattering at 25 °C, which is below the transition temperature for all mutants, was normalized to zero prior to analysis of the data. The measurements (duplicates or triplicates for all proteins) were quite reproducible, as shown, as an example, by the three measurements of the scFv fragment A48^{--}(H1), performed on different days (Figure 5c). The error bars in Figure 5d indicate the upper and lower extremes of duplicate or triplicate measurements.

The aggregation temperatures averaged from these measurements were between 45.1 °C for A48^{--}(H2) and 70.8 °C for scFv A48^{++}(H2L1). The fragments A48^{--}(H1) and A48^{--}(H2) had similar aggregation temperatures. The additional H-N52S mutation in A48^{--}(H2) apparently caused a decrease of about 2 °C in the aggregation temperature, while the same mutation had caused a shift to higher urea denaturation midpoints (Figure 5a, Table 1). The A48^{-+}(H1) and A48^{--}(H3L1) fragments showed identical averaged aggregation temperatures of 53.0 °C, consistent with their similar denaturation midpoints. The interface-bridged variant A48^{--}(H2)(SS) had its onset of aggregation at 55.0 °C. Significantly higher denaturation temperatures of 63.2 °C (A48^{++}) and 70.8 °C [A48^{++}(H2L1)] were observed for the two cysteine-restored variants. Overall, a good correlation (correlation coefficient 0.97) was found between the denaturation midpoints in urea unfolding and the aggregation temperatures identified, when comparing all seven scFv fragments (Figure 5d).

We have to point out, however, that the *x* values in Figure 5d are not completely unambiguous. Especially in the mutants with two obvious transitions, like A48^{++}(H2L1) or, less pronounced, A48^{++}, one would, strictly speaking, have to take the midpoint of the first transition of the denaturation curve for use in Figure 5d, as the protein loses its function there. However, the change from a clear two-step transition to a clear one-step transition in the equilibrium denaturation curves is gradual. A classification of the scFv fragments into two groups, where either the midpoint of the entire transition or of the first "step" of the transition is taken as a semiquantitative measure of stability would therefore be arbitrary. We thus decided to use the midpoint of the entire transition in all cases, even if the transitions are clearly not two-state.

Analytical Gel Filtration. After 20 h of incubation at 37 °C only the two least stable variants A48^{--}(H1) and A48^{--}(H2) showed a significant decrease in the amount of remaining monomeric protein (open circles, Figure 6a). For all other scFv fragments, more than 80% was still monomeric protein. Apparently, the incubation time of 20 h was not long enough to distinguish between the more stable scFv fragments. Interestingly, only 1.7% of A48^{--}(H2) was monomeric after 20 h at 37 °C, while 30.1% of A48^{--}(H1) survived the same treatment as monomeric species. Therefore, these gel filtration data reflect the slightly lower aggregation temperature measured for the scFv fragment A48^{--}(H2) compared with A48^{--}(H1), while they do not correspond to the higher denaturant midpoint of A48^{--}(H2). Apparently, the mutation H-N52S is stabilizing in equilibrium urea denaturation but negatively influences the aggregation behavior upon heating the protein.

When the incubation time at 37 °C was extended to 120 h, more of the mutants could be compared, as they were no longer all stable and the proportionality range in the plot of aggregation temperature versus monomeric protein was shifted to higher aggregation temperatures (filled triangles, Figure 6a). After 120 h at 37 °C, only the cysteine-restored variants were still more than 90% monomeric, whereas in all other variants, less than 40% of scFv protein remained monomeric. On the other hand, a discrimination between the two least stable scFv fragments A48^{--}(H1) and A48^{--}(H2) was now no longer possible, because both these proteins were completely aggregated after 120 h incubation at 37 °C, while they could still be distinguished after 20 h of incubation. A representative set of gel filtration chromatograms is shown in Figure 6b. The overlay of the curves obtained for the fragment A48^{-+}(H1) without incubation at 37 °C and after 20 and 120 h of incubation at 37 °C demonstrates that the aggregation peak did not increase proportionally to the decrease of the peak representing monomeric scFv fragment, most likely because larger aggregates were removed by centrifugation before all gel filtration runs.

The urea unfolding midpoints, the averaged aggregation temperatures from duplicate or triplicate measurements, and the percentage of monomeric protein after 20 and 120 h of incubation at 37 °C are summarized for the seven analyzed A48 scFv fragments in Table 1.

DISCUSSION

On basis of the different shapes of the denaturant-induced equilibrium unfolding curves and on the interpretation of the fluorescence spectra, which can be assigned to denatured, native, and assembled domains (*27*), we propose a classification of scFv fragments regarding the relative stability

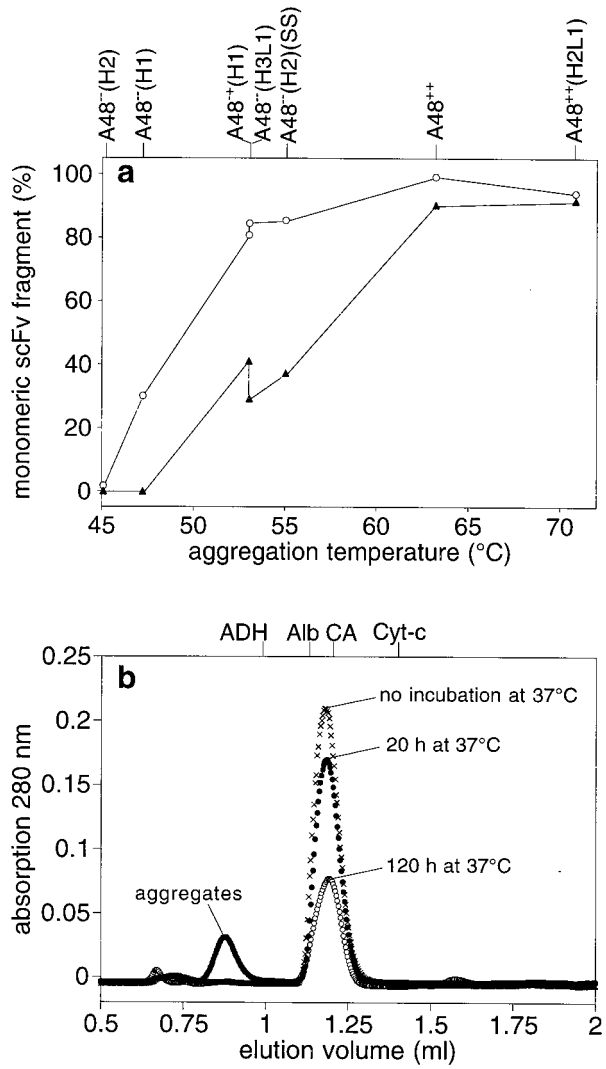

FIGURE 6: Thermal aggregation of different A48 scFv fragments after prolonged incubation at 37 °C. (a) Correlation between the aggregation temperature and the percentage of monomeric scFv fragment remaining after 20 h incubation at 37 °C (○) or 120 h (▲), respectively. The amount of monomeric protein was quantified by integrating the peak representing monomeric scFv fragment which eluted from a Superdex-75 analytical gel filtration column. (b) As a representative example, an overlay of the analytical Superdex-75 gel filtration chromatograms of A48^{-+}(H1) without incubation (×) and after 20 (●) and 120 (○) h of incubation at 37 °C is shown. Monomeric scFv eluted at about 1.2 mL. The amount of remaining monomeric species decreased with increasing incubation time. Elution volumes of molecular mass marker proteins are indicated: alcohol-dehydrogenase (ADH) (150 kDa), bovine serum albumin (Alb) (66 kDa), carbonic anhydrase (CA) (29 kDa), and cytochrome *c* (cyt-*c*) (12.4 kDa).

of V_L, V_H, and the interface. We will discuss in detail examples for the different classes, and we also show how the stability of a scFv fragment can be increased, once it has been grouped into one of the proposed classes, by identifying and then improving the stability limiting part.

First proposed by Brands and co-workers (*29*) and discussed previously (*9*), the total stability of a domain A in a two-domain protein AB, such as an scFv fragment, is the sum of the intrinsic stability of A and the stabilizing contribution of the interface. The intrinsic stability is the stability in the absence of any interacting domain. Different extreme cases can be envisaged, depending on the relative intrinsic stabilities of the isolated V_H and V_L domains in an scFv fragment, the stabilizing contribution of the interface, and the stability of the entire scFv fragment.

The basis for the classification is the interpretation of the fluorescence spectra of antibody domains. They are essentially governed by the intrinsic tryptophan fluorescence, even when excited at 280 nm, since the absorbance at 280 nm and the quantum yield of emission of tyrosine and phenylalanine is much lower than the respective values for tryptophan (*30*), and since the compact folded state of native proteins allows efficient nonradiative energy transfer from phenylalanine to both tryptophan and tyrosine and from tyrosine to tryptophan residues (*31*). From the study of single domains and their association (*9*, *27*), a few general conclusions can be drawn. V_L in general carries a single conserved Trp at position L35. This is almost completely quenched in the native state and thus contributes very little to the spectrum of a native scFv. In contrast, V_H usually has 4−5 Trp residues, one of them at the corresponding position H36, the others at positions quite solvent exposed in the isolated V_H domain. Since this Trp H36 contributes only a small fraction to the fluorescence of native V_H, the observed red-shift in fluorescence emission maximum upon denaturation of an isolated V_H domain is usually only a few nanometers (*9*, *27*). In the case of disulfide-free variable domains, the quenching of Trp L35 upon folding is less pronounced, resulting in an enhancement of fluorescence intensity of this deeply buried residue in the native state, which shifts the entire emission maximum of the scFv fragment to a discernible lower wavelength. When V_H and V_L form a complex, some Trp residues (usually around 3, the ones at position H47 and H103 being highly conserved) become buried in the interface, and thus, their emission maximum is shifted to lower wavelength.

It is also customary to analyze equilibrium transitions by following the fluorescence intensity, for example at 350 nm (*8*). An increase in the fluorescence intensity at 350 nm upon denaturation of V_L (*9*, *27*), an increase (*27*) or decrease (*9*) upon denaturation of V_H, and a slight decrease (*27*) upon disruption of the interface can be observed. These intensity changes are, however, strongly scFv dependent, and general predictions about their amplitude and direction are therefore not possible. In addition, the denaturation of one of the domains of the scFv fragment will in most cases happen simultaneously with interface disruption (with the exception of case IV, see below). Therefore, the changes in intensity at 350 nm can mutually compensate each other. Note that this effect is not observed when fluorescence emission maximum data are analyzed, because here all three processes (denaturation of V_H, V_L, and interface disruption) cause a change of the emission maximum to higher wavelength, i.e., in the same direction (see below), albeit by only small amounts for some transitions. Nevertheless, in some cases, the intensity data may give supporting information about equilibrium intermediates and can corroborate the occurrence of two-state transitions.

In our experiments, we estimate thermodynamic stabilities from the urea denaturation transitions only semiquantitatively by giving the midpoints of the unfolding curves. As is well-known, one can derive ΔG values from unfolding curves (*32*), but a necessary prerequisite for this procedure is that the unfolding follows the two-state model or that the curve can clearly be broken down in several two-state processes.

In the present set of scFv fragments, however, this prerequisite is clearly not fulfilled for most of the mutants. In the two-state model, the *m*-value, which describes the steepness of the transition curve, also affects the calculation of free energies, by affecting the extrapolation to zero denaturant (*33*). However, in our scFv fragments, the steepness is influenced in most cases by the fact that the two domains of the scFv fragment do not unfold cooperatively, but one after the other, even if no obvious step is visible in the unfolding curve, such as, for example, described for the A48^{--}(H2) scFv fragment above. This observation may actually apply to many scFv fragments, in which case calculations of ΔG values are not appropriate, and we suggest to give only the denaturation midpoints as semiquantitative stability estimates. Moreover, deriving free energies from fluorescence emission maximum curves is problematic in general, because this may only be adequate when the fluorescence emission maximum changes proportionally with the population of macrostates, i.e., when it reflects the mole fraction of native and denatured molecules. This will only be the case if the quantum yield of native and denatured states is the same (*8*).

In the present classification, we refer to the domains as V_A and V_B, where either one can be V_H or V_L. Thus, the classification is based on relative stability of V_A versus V_B, and we define V_A as the intrinsically more stable domain. Thus, there can be two subcases, one where V_A is V_H, the other where V_A is V_L, and V_B is the respective partner.

Classes of ScFv Fragments. In class I (Figure 3), the intrinsic stability of one domain is significantly higher than the total stability (intrinsic plus extrinsic contribution) of the other domain. Consequently, an unfolding intermediate will accumulate at equilibrium, where one domain is completely unfolded while the other domain is still native. A visible step in the unfolding curve is one indication for this kind of scFv fragments. This step in the fluorescence emission maximum representation will be relatively large and easy to make out if V_L denatures earlier than V_H, mainly due to the interface Trp residues of V_H (see above) which become solvent-exposed upon denaturation of V_L.

If V_H denatures before V_L, however, the step will usually be much more difficult to discern, because V_L has often only one Trp residue (see above), and therefore the further shift in the fluorescence emission maximum caused by denaturation of V_L in the presence of an already denatured V_H will be relatively small. The exact size of the observed step will vary from scFv to scFv and be mainly dominated by the amount and position of the Trp residues in V_H and V_L. An important piece of further experimental evidence for such an equilibrium intermediate with one domain being native and the other being unfolded is that the denaturation of the isolated more stable domain will occur at the same denaturant concentration as the second step in the scFv unfolding curve (*9*). Moreover, limited thermolysin digestion (*9*, *24*) of the scFv at the particular denaturant concentration where the intermediate is expected, based on the unfolding curve, should result in the accumulation of a stable core fragment comprising the more stable scFv domain.

In class II (Figure 3), the intrinsic stability of one domain is in the same range as the total stability of the other domain. This means that the interface has increased the total stability of the weaker domain to almost the same level as the stability of the stronger domain. No step will be detectable in the equilibrium unfolding curve based on the emission maximum. However, the transition region can be conspicuously gradual, which is a consequence of the two domains unfolding one right after the other. Therefore, the transition may only seemingly be two-state, but is actually a superposition of two transitions occurring quite close together. Any minor further stabilization of the intrinsically more stable domain will result in a step in the denaturation curve and therefore lead to class I.

ScFv fragments falling into class III (Figure 3) consist of two domains of relatively low intrinsic stability which are linked by a very stable interface. In this situation, the transition of the entire scFv fragment in equilibrium unfolding takes place much later than the transition of either isolated domain. Each domain provides extrinsic stabilization to the partner domain, and an early disruption of the interface, which would leave the domains only with their low intrinsic stabilities, is prevented. Because of the low intrinsic stabilities of the isolated domains, the breaking up of the V_H-V_L interface is necessarily linked to the immediate denaturation of the isolated domains, which are already far above their intrinsic stability at the denaturant concentration where the interface disrupts. A steep transition of the unfolding curve—in this case describing a real two-state transition—and transition curves of the isolated domains with transitions at much lower denaturant concentration than the curve of the scFv fragment are experimental evidence for this kind of behavior.

A further case one might postulate is class IV (Figure 3). In this situation, two intrinsically very stable domains are linked by a weak interface. The breaking up of the V_H-V_L interface will occur at lower denaturant concentration than the denaturation of either of the domains. The order of their subsequent denaturation will solely depend on the relative intrinsic stabilities of V_H and V_L. Although we could not find any scFv fragment belonging to class IV so far, we should be able to predict how such a denaturation curve should look like. The processes, disruption of the interface, denaturation of V_H, and denaturation of V_L will all result in a red-shift of the fluorescence emission maximum, because Trp residues, which were in the hydrophobic interface region or in the interior of the domains in the native protein, will then become solvent exposed. Therefore, the first step in the fluorescence emission maximum transition should be caused by disruption of the interface and subsequent exposure of the V_H Trp residues positioned in the interface region. The resulting spectrum would be the computational addition of the spectra of V_L^N and V_H^N. The first step will be followed by a second and perhaps third step in the denaturation curve, depending on whether the V_H and V_L domain happen to denature at the same denaturant concentration or differ in their intrinsic stability. In class IV, in contrast to class I, the first transition should occur at lower denaturant concentration than the transition of either isolated domain.

Examples of ScFv Fragments for the Different Classes. One scFv fragment which can be placed into class I (Figure 3) is A48^{++}(H2) [A48cys(H-K66R/N52S)], whose unfolding equilibrium intermediate with native V_H and denatured V_L has been described in detail before (*9*). The same relationship—the intrinsic stability of V_H being significantly higher than the total stability of V_L—is also found in the scFv fragment A48^{--}(H3) (Figure 2a) described in this study. In this

mutant, we see a clear step in the fluorescence emission maximum unfolding curve, representing such a defined equilibrium intermediate.

An example of the reciprocal case, where the intrinsic stability of V_L is significantly higher than the total stability of V_H and where an equilibrium intermediate with native V_L and denatured V_H accumulates at equilibrium at about 2−2.5 M GdnHCl concentration, is the 4D5 scFv fragment. We have described the urea unfolding of this scFv fragment before (*14*), without being aware of such an intermediate. The reason for this is that even at the highest urea concentration used in our previous experiment (9 M), the unfolding of V_L had probably not completely occurred yet. Only with GdnHCl as a much stronger denaturant the second transition becomes apparent—even though it is very hard to make out in the unfolding curve by monitoring the fluorescence emission maximum (Figure 2b), for the reasons mentioned above. However, corroborating evidence could be obtained by limited thermolysin digestion, similar to the reciprocal case with native V_H and denatured V_L in $A48^{++}$(H-K66R/N52S), observed at 6 M urea before (*9*). Limited thermolysin digestion of the 4D5 scFv fragment in the presence of 2 M GdnHCl resulted in the accumulation of initially two main bands which both contain the entire V_L domain, and, after very long digestion convert into one main fragment (Figure 4). This underlines that the V_L domain of the 4D5 scFv fragment is indeed structured under these conditions, while V_H is not. Further evidence for the equilibrium intermediate present in the scFv fragment 4D5 at 2 M GdnHCl comes from kinetic experiments showing that 4D5 scFv fragment refolded from 2 M GdnHCl is lacking the slow Pro-isomerization limited phase, suggesting that the Pro L95 is still in a cis configuration at 2 M GdnHCl. This demands that the 4D5 V_L domain must still be native under these conditions (*34*).

An example for a scFv fragment where the intrinsic stability of one domain is in the same range as the total stability of the other domain and which can therefore be placed into class II (Figure 3) is $A48^{--}$(H2). As seen in Figure 2a this scFv fragment has a conspicuously flat transition curve. Evidence for the fact that this transition is actually a superposition of two transitions occurring close together, first V_L, then V_H, comes from the fact that a step becomes apparent in the unfolding curve of the scFv fragment, as soon as the V_H domain in this scFv fragment is further stabilized by introducing the additional V_H mutation Y-92V. The same situation applies to $A48^{++}$ described previously (*9*), since in this scFv fragment the flat transition curve is also resolved into a clear two-step transition, represented by a step in the denaturation curve, as soon as the already slightly more stable V_H domain is further stabilized by introducing the mutation H-K66R.

Finally, we want to give an example for class III (Figure 3), the situation where two intrinsically quite unstable domains are linked by a very stable interface. We have created such a molecule in the case of the interface disulfide-bridged variant $A48^{--}$(H2)(SS). The midpoint of its transition is at 4.7 M urea (Figure 2d). The corresponding isolated V_L domain, however, even *with* the disulfide bridge, denatures with a midpoint at 2.3 M urea, as analyzed previously (*9*). The disulfide-free one would be even significantly less stable, and expression by itself was not feasible at all. The $A48V_H^-$(H2) domain, which is part of this scFv, has a denaturation midpoint at 3.3 M urea, which is also clearly earlier than the $A48^{--}$(H2)(SS) scFv transition. It can be noticed that the $A48^{--}$(H2)(SS) has indeed a rather steep transition curve and represents probably the only scFv fragment among the A48 mutants analyzed here which has a two-state unfolding behavior.

Predictions of how the corresponding scFv fragments can be further stabilized can immediately be derived from the classification of a given scFv fragment. The $A48^{++}$(H2) scFv fragment could, for example, be stabilized by introducing the V_L stabilizing mutation L-T8P, creating the scFv fragment $A48^{++}$(H2L1), because V_L was (and still is) limiting for the stability of this scFv fragment (Figure 2b, open circles). The identical situation applies to $A48^{--}$(H3) (Figure 2a). Here, the addition of the L-T8P mutation also caused a shift of the first part in the unfolding curve, representing the V_L transition, to higher denaturant concentrations (Figure 2a, closed squares), thereby stabilizing the scFv fragment.

The 4D5 scFv fragment, on the other hand, can only profit from stabilizing its V_H domain, which is clearly limiting for the stability of this scFv fragment. In fact, we could create the extremely stable "hybrid" scFv fragment, denaturing with an unfolding midpoint of 3.0 M GdnHCl, by genetically linking the very stable V_L domain of the scFv fragment 4D5 to the very stable V_H domain of scFv $A48^{++}$(H2) (Figure 2b). This "hybrid" scFv fragment, although not binding any antigen at present, may be a very suitable acceptor in CDR grafting experiments (Wörn et al., manuscript in preparation). Besides its extraordinary stability it is also very well expressed.

To prove the more or less additive effect of intrinsic and extrinsic stability contributions further, we have inserted an interface disulfide bond into the "hybrid" scFv fragment. This disulfide bond did, as seen in Figure 2b, indeed cause a further shift of the GdnHCl denaturation curve to higher concentrations, because the two domains are now "forced" to remain associated longer, providing more extrinsic stabilization to the partner domain. The "hybrid" (SS) scFv fragment remained native up to about 7 M urea (Figure 2c). The dramatically decreased purification yield of the periplasmically expressed interface-bridged variant "hybrid" (SS) scFv, however, was to be expected (*35*), because the additional two cysteines H44 and L100 will allow the formation of multiple incorrectly disulfide bridged variants in the oxidizing environment of the periplasm.

ScFv fragments belonging to class IV (Figure 3), if they occurred, could clearly be stabilized by stabilizing the V_H-V_L interface, possibly by introducing an interface−disulfide bond. It may be more difficult to gain further stabilization of scFv fragments with domains of low intrinsic stability, linked by a very stable interface (class III in Figure 3), because one of the domains would have to be stabilized significantly to provide further extrinsic stabilization to the other domain.

While it may sometimes be difficult to group any given scFv fragment into one of the proposed classes, especially since the borderlines are often not that clear, we believe that such a classification is very useful for increasing the stability of a scFv fragment. Clearly, the prerequisite for such an undertaking is the knowledge, which part of the scFv is limiting for its stability and therefore needs to be improved.

Correlation between Urea Denaturation Midpoints and Aggregation Properties. The strong overall correlation between the midpoint in urea denaturation and the aggregation temperature observed in the seven mutants of the A48 scFv fragment investigated is in agreement with similar results described for other model systems. Chrunyk and Wetzel (*25*) investigated the relationship between aggregation temperature and thermodynamic stability in different Interleukin-1β point mutants and also found a general proportionality, although one mutation resulted in a protein aggregating 7 °C lower than expected from its thermodynamic stability. A similar situation in the A48 scFv fragment model system is observed in the case of the H-N52S mutation, which stabilizes the protein during equilibrium unfolding in urea, causing a shift of the transition curve to higher urea concentration, but slightly decreases the aggregation temperature. The mechanistic reason for this discrepancy, however, cannot be extracted from our experiments.

With our model system, we can show that the overall strong correlation of aggregation temperature and urea unfolding behavior seems to be valid over a wider range of stabilities than ever tested before. While the eight Interleukin-1β variants investigated by Chrunyk and Wetzel all aggregated within a window of 6 °C (*25*), the most stable and the least stable A48 scFv mutants investigated here differ in their aggregation temperature by 25.7 °C. Moreover, the long-term stability against aggregation at 37 °C, monitored by analytical gel filtration, is also closely linked to the actual aggregation temperature determined by light scattering.

In many proteins, partially unfolded intermediates expose hydrophobic parts, which are buried in the native structure and are believed to be responsible for aggregation (*36*−*40*). These intermediates may be populated in equilibrium unfolding transitions, but they are kept in solution by the action of the denaturant (*36*), which may directly interact with the protein and influence the properties of the solvent. Therefore, a correlation between thermodynamic stability and aggregation temperature would require that the intrinsic aggregation rate of the intermediate is about the same for the mutants and that the mutations only influence under which environmental conditions (temperature or denaturant) this intermediate is significantly populated. However, the overall rate of aggregation and the temperature influence may also depend on the aggregation rate of the intermediate itself. In addition, single mutations may act by favoring non-native interactions that stabilize aggregates, without necessarily decreasing the thermodynamic stability of the native protein. The possible effects of single mutations on the mechanism of aggregation are comprehensively reviewed in ref *41*.

In summary, our studies demonstrate that thermodynamic stabilities and thermal aggregation correlate well for the scFv fragments investigated. Thus, measuring scFv stabilities by analyzing denaturation induced unfolding curves and their interpretation as detailed here may turn out to be a good predictor for scFv stabilities during in vivo applications and pave the way to highly robust antibody fragments. Indeed, an improved in vivo performance of a scFv fragment with increased in vitro stability has been reported for a mutant scFv fragment derived from the mAb B3 (*6*) and for a stabilized version of the MOC31 scFv fragment (Willuda et al., manuscript submitted for publication). However, we have to qualify that "stability" of a scFv fragment in the human body, defined as functional half-life, is undoubtedly much more complicated and will not only be influenced by thermal aggregation but also by proteolysis, blood clearance and other effects. It is a very important challenge to understand the molecular basis of these different contributions in the future.

REFERENCES

1. Bird, R. E., Hardman, K. D., Jacobson, J. W., Johnson, S., Kaufman, B. M., Lee, S. M., Lee, T., Pope, S. H., Riordan, G. S., and Whitlow, M. (1988) *Science 242*, 423−426.
2. Huston, J. S., Levinson, D., Mudgett-Hunter, M., Tai, M., Novotny, J., Margolies, M. N., Ridge, R. J., Bruccoleri, R. E., Haber, E., Crea, R., and Oppermann, H. (1988) *Proc. Natl. Acad. Sci. U.S.A. 85*, 5879−5883.
3. Plückthun, A., Krebber, A., Horn, U., Knüpfer, U., Wenderoth, R., Nieba, L., Proba, K., and Riesenberg, D. (1996) in *Antibody Engineering, A Practical Approach* (McCafferty, J., Hoogenboom, H. R., and Chiswell, D. J., Eds.) pp 203−252, IRL press, Oxford University Press, New York.
4. Glockshuber, R., Malia, M., Pfitzinger, T., and Plückthun, A. (1990) *Biochemistry 29*, 1362−1367.
5. Bregegere, F., England, P., Djavadi-Ohaniance, L., and Bedouelle, H. (1997) *J. Mol. Recognit. 10*, 169−181.
6. Behar, I., and Pastan, I. (1995) *J. Biol. Chem. 270*, 23373−23380.
7. Pace, C. N., Shirley, B. A., and Thomson, J. A. (1989) in *Protein Structure, A Practical Approach* (Creighton, T. E., Ed.) pp 311−330, IRL-Press, Oxford University Press.
8. Eftink, M. R. (1994) *Biophys. J. 66*, 482−501.
9. Wörn, A., and Plückthun, A. (1998) *Biochemistry 37*, 13120−13127.
10. Rudikoff, S., and Pumphrey, J. G. (1986) *Proc. Natl. Acad. Sci. U.S.A. 83*, 7875- 7878.
11. Proba, K., Honegger, A., and Plückthun, A. (1997) *J. Mol. Biol. 265*, 161−172.
12. Proba, K., Wörn, A., Honegger, A., and Plückthun, A. (1998) *J. Mol. Biol. 275*, 245−253.
13. Kelley, R. F., O'Connell, M. P., Carter, P., Presta, L., Eigenbrot, C., Covarrubias, M., Snedecor, B., Bourell, J. H. and Vetterlein, D. (1992) *Biochemistry 31*, 5434−5441.
14. Wörn, A., and Plückthun, A. (1998) *FEBS Lett. 427*, 357−361.
15. Kabat, E. A., Wu, T. T., Perry, H. M., Gottesman, K. S., and Foeller, C. (1991) *NIH Publication No. 91-3242*, National Institute of Health, Bethesta, MD.
16. Spada, S., Honegger, A., and Plückthun, A. (1998) *J. Mol. Biol. 283*, 395−407.
17. Brinkmann, U., Reiter, Y., Jung, S.-H., Lee, B., and Pastan, I. (1993) *Proc. Natl. Acad. Sci. U.S.A. 90*, 7538−7542.
18. Ge, L., Knappik, A., Pack, P., Freund, C., and Plückthun, A. (1995) in *Antibody Engineering* (Borrebaeck, C. A. K., Ed.) 2nd ed., pp 229−266, IRL Press, Oxford University Press.
19. Freund, C., Ross, A., Guth, B., Plückthun, A., and Holak, T. A. (1993) *FEBS Lett. 320*, 97−100.
20. Studier, F. W., and Moffatt, B. A. (1986) *J. Mol. Biol. 189*, 113−130.
21. Knappik, A., Krebber, C., and Plückthun, A. (1993) *Biotechnology 11*, 77−83.
22. Knappik, A., and Plückthun, A. (1994) *Biotechniques 17*, 754−761.
23. Tang, Y., Jiang, N., Parakh, C., and Hilvert, D. (1996) *J. Biol. Chem. 271*, 15682−15686.
24. Heinrikson, R. L. (1977) *Methods Enzymol. 47*, 175−189.
25. Chrunyk, B. A., and Wetzel, R. (1993) *Protein Eng. 6*, 733−738.
26. Cowgill, R. W. (1967) *Biochem. Biophys. Acta 140*, 37−41.
27. Jäger, M., and Plückthun, A. (1999) *J. Mol. Biol. 285*, 2005−2019.
28. Schmid, F. X. (1997) in *Protein Structure, A Practical Approach* (Creighton, T. E., Ed.) 2nd ed., pp 261−297, IRL Press, Oxford University Press.

29. Brandts, J. F., Hu, C. Q., and Lin, L. N. (1989) *Biochemistry 28*, 8588−8596.
30. Eftink, M. R. (1991) in *Methods of biochemical analysis* (Suelter, C. H., Ed.) Vol. 35, J. Wiley, New York.
31. Cantor, C., and Schimmel, P. R. (1980) *Biophysical Chemistry*, Vol. II, pp 433−465, Freeman, W. H., San Francisco.
32. Pace, C. N. (1990) *Trends Biotechnol. 8*, 93−98.
33. Pace, C. N. (1986) *Methods Enzymol. 131*, 266−289.
34. Ramm, K., and Plückthun, A. (1999) *J. Mol. Biol.* (in press).
35. Young, N. M., MacKenzie, C. R., Narang, S. A., Oomen, R. P., and Baenziger, J. E. (1995) *FEBS Lett. 377*, 135−139.
36. Fink, A. L. (1998) *Folding Des. 3*, R9−23.
37. Mitraki, A., and King, J. (1989) *Biotechnology 7*, 690−697.
38. Wetzel, R. (1996) *Cell 86*, 699−702.
39. Wetzel, R. (1992) in *Protein Engineering, A Practical Approach* (Rees, A. R., and Sternberg, M. J., Eds.) pp 191−219, IRL Press, Oxford University Press.
40. Kim, D., and Yu, M. H. (1996) *Biochem. Biophys. Res. Commun. 226*, 378−384.
41. Wetzel, R. (1994) *Trends Biotechnol. 12*, 193−198.

BI9902079